



Direct Numerical Simulation of a Mixed-Media Model for Efficient Developing Shale Gas Reservoirs

Ning Li^{1,2}(✉) and Lin Yan^{1,2}

¹ Research Institute of Petroleum Exploration and Development, PetroChina, Beijing, China

lining_riped@petrochina.com.cn

² National Energy Tight Oil and Gas R&D Center, Beijing, China

Abstract. Unconventional shale gas reservoirs have developed nanometer-scale matrix pores with extremely low permeability, complicated gas occurrence states and migration mechanisms, and it is difficult to effectively be developed by conventional gas field development technologies. Under the applications of horizontal wells and volume fracturing technology application, multiple scale matrices and fracture media are generated and staggered. It is difficult to accurately describe the flow of fractured media using continuum media models. Aiming at the key technical issues in the efficient development and numerical simulation of shale gas reservoirs, this paper systematically analyzes the relevant adsorption/desorption mechanisms and laws of shale gas, builds a mixed-media model based on discrete fractures, and builds a set of mathematical models of shale gas nonlinear migration based on considering adsorption / desorption mechanism. A suite of numerical discrete equations based on an unstructured grid was formed. A direct numerical simulator for shale gas based on mixed-media model was developed. After fully verifying the functional reliability of the simulator by comparing with commercial simulator, a case of direct numerical simulation of shale gas reservoirs based on mixed-media model with complex migration mechanisms was carried out. From the numerical simulation results, it can be seen that the mixed media simulation technology can effectively simulate the complex flow of shale gas. This technology is suitable for direct numerical simulation calculation of shale gas development, and provides a powerful numerical simulation means for gas field development researcher.

Keywords: Shale gas · Discrete fracture · Migration mechanism · Reservoir simulation

1 Introduction

As a clean and efficient energy source, natural gas is the representative of a low-carbon economy. Large-scale development and utilization of natural gas resources is a realistic choice to deal with global warming. The average predicted value of available natural gas resources in the world is 458.7×10^4 billion cubic meters [1], which is 150 times the current average annual global natural gas consumption. The lowest and highest

predicted values are 351.1×10^4 billion cubic meters and 598.0×10^4 billion cubic meters, respectively.

As an unconventional natural gas, shale gas is becoming a force that affects the world energy market. This kind of gas, which the international energy community calls “game changers”, has greatly rewritten the world’s energy landscape. At present, the United States has successfully carried out industrial shale gas mining in the country, and gradually formed a set of advanced shale gas exploration and development technologies. This achievement, called as a “shale gas revolution”, not only greatly changed the supply of natural gas in North America, but also set off a booming of developing shale gas worldwide [2, 3]. Figure 1 is the historical output and predicted value of national natural gas given by the US Energy Information Administration in 2020 [4]. In the AEO2020 reference case, natural gas production from shale gas and tight oil extraction continues to grow, accounting for the total US natural gas production. Both proportion and absolute volume are increasing. The reason for the increase is the scale of related resources (nearly 500,000 square miles) and technological advances that allow these resources to be developed at a lower cost. In the “high oil and gas supply” case with more optimistic assumptions about resource scale and recovery, the cumulative production of shale gas and tight oil is 14% higher than the reference case. On the contrary, in the case of “oil and gas shortage”, the cumulative output of these resources is 20% lower than the output in the reference case.

In recent years, major breakthroughs have been made in the exploration of shale gas reservoirs in China, with resources exceeding 45 trillion cubic meters and preliminary estimates of recoverable reserves of approximately 31 trillion cubic meters. However, due to China’s current rapid economic development and rapid increase in demand for energy, it is expected that by 2030, China's natural gas gap will exceed 130 billion cubic meters [5]. Therefore, there is an urgent need to realize the effective development of shale gas reservoirs, promote the rapid development of the natural gas industry, and meet the national energy demand.

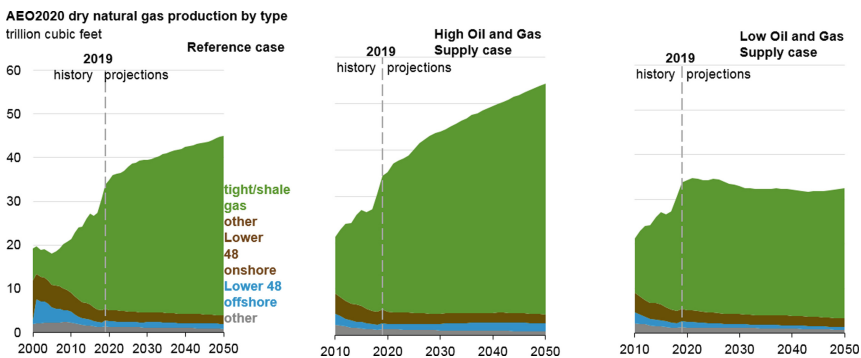


Fig. 1. US natural gas production and forecast.

However, due to the Nano scale pores in the shale reservoir, the extremely low permeability of the reservoir matrix, and the complex gas occurrence and migration

mechanism, it is an unconventional gas reservoir. The fracture network is complicated after hydraulic fracturing, and accurate numerical simulation is difficult. Shale reservoirs include rock matrix, organic matrix with kerogen, natural fractures, and artificial hydraulic fractures. The scale of various media is different, the scale of pore diameter ranges from nanometers to micrometers, and the scale of fracture aperture ranges from micrometers to millimeters. The involved mechanisms are very complex, including: desorption/adsorption, diffusion, slippage, Darcy flow and non-Darcy flow, matrix pores will deform and shrink with pressure changes, and fractures will deform and be closed; There are coupling of medium, coupling of fluid pattern, coupling of different scale, coupling of fluid migration and stress, and the mechanism of migration of different media at different times and times changes, as shown in Fig. 2.

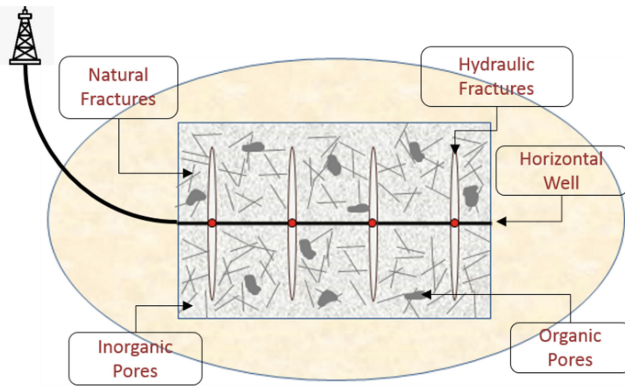


Fig. 2. Schematic diagram of complex coupled migration of shale gas reservoirs.

Faced with many problems in the current development process of shale gas reservoirs, the reservoir numerical simulation method can more fully consider the coupling of various processes such as seepage, diffusion, desorption, and pressure sensitivity during shale gas migration [6, 7]. An accurate mathematical model can provide effective simulations for shale gas reservoir selection evaluation, dynamic analysis, productivity estimation, and hydraulic fracturing measures design. There are two difficulties in the simulation of shale gas. The first is to establish a suitable mathematical model of adsorption/desorption mechanism, which needs to conform to the law curve of desorption/adsorption obtained from the laboratory. The second is the simulation technology for matrix-fracture-wellbore together. The simulation technology of mixed media needs to conform to the flow laws of shale gas in the matrix, fractures and wellbore system. Therefore, this paper focuses on two difficulties and conducts targeted numerical simulation research on the shale gas development process.

2 Governing Equation

For the simulation of shale gas, the first thing that needs to be done is to establish a mathematical model that can correctly describe the state of shale gas flow underground. The mathematical model of shale gas numerical simulation needs to meet the following conditions: 1) Since 80% of shale gas is adsorbed on the rock surface in an adsorbed state, when the gas reservoir pressure is lower than the desorption pressure, a large amount of desorbed gas becomes free, and at the same time, since shale gas development must adopt hydraulic fracturing volume reconstruction technology, there will be a large amount of water phases in the gas reservoir, so the gas and water two phases are considered in the gas reservoir; 2) rock and water are slightly compressible; 3) consider the anisotropy and heterogeneity of the stratum, as well as the influence of gravity and capillary force.

For any microelement in the reservoir, whether it is fracture medium or matrix medium, whether it is continuous medium or discrete medium, the following mathematical model equations need to be established:

$$\frac{\partial}{\partial t}(\phi\rho_g S_g + m_k) = -\nabla \cdot (\rho_g \mathbf{v}_g) + q_g \quad (1)$$

$$\frac{\partial}{\partial t}(\phi\rho_w S_w) = -\nabla \cdot (\rho_w \mathbf{v}_w) + q_w \quad (2)$$

$$S_g + S_w = 1 \quad (3)$$

$$P_g - P_w = P_{cwg} \quad (4)$$

Where, ϕ is the porosity, %; ρ_g and ρ_w is the density of the gas and water phases under formation conditions respectively, kg/m^3 ; S_g and S_w is the saturation of the gas and water phases respectively, %; m_k is the mass of gas adsorbed and desorbed per unit volume of the reservoir, kg; P_g and P_w is the pressure of the gas phase and the water phase respectively, MPa; P_{cwg} is the capillary force between the gas and water phase, MPa; q_g and q_w is the production / injection volume between the gas phase, the aqueous and the wellbore respectively, kg; \mathbf{v}_g and \mathbf{v}_w is the gas phase and the water phase flow rate respectively, m/s.

According to Darcy's law formula, the velocity of phase p ($p = g, w$) can be expressed as:

$$\mathbf{v}_p = -\frac{KK_{rp}}{\mu_p}(\nabla\Phi_p) \quad (5)$$

Where, K is the absolute permeability, mD; K_{rp} represents the relative permeability of the phase p , dimensionless; μ_p is the viscosity of the phase p , $\text{Pa} \cdot \text{s}$; Φ_p is the flow potential of phase p , which can be expressed as:

$$\nabla\Phi_p = (\nabla P_p - \rho_p g \nabla D) \tag{6}$$

Where, g is the acceleration of gravity, m/s^2 ; D is the depth from the reference plane, m .

3 Numerical Discretization

The integral finite difference method is used to discretize the control equation. The integral finite difference method was proposed by Narashman et al. [8] in 1976 and is a more effective method for solving the underground gas-water flow. It combines the advantages of the finite difference method and the finite element method. On the one hand, the difference method is used to discretize, and on the other hand, the irregular grid is used to deal with the boundary and grid problem, which overcomes the natural boundary fitting when solving with the finite difference. At the same time, because the integral finite difference method is derived from the physical concept of the fluid balance of the unit body, the basic equations are derived, which ensures the conservation of fluid flow in the unit domain. The discrete equation is:

$$\frac{V_i}{\Delta t} \left[(\phi\rho_p S_p)_i^{n+1} + (m_k)_i^{n+1} - (\phi\rho_p S_p)_i^n - (m_k)_i^n \right] = \sum_{j \in \eta_i} F_{p,ij}^{n+1} + Q_{p,i}^{n+1} \tag{7}$$

Where, the superscript n represents the last time step, $n + 1$ is the current time step; The subscript i represents the grid node i , and its value range is $i = 1, 2, 3, \dots, N$, N represents the total number of grid node; Δt is the time step size, s ; V_i is the volume of node i , m^3 ; η_i is the set of neighboring node j of node i ; $(m_k)_i^{n+1}$, $F_{p,ij}^{n+1}$, $Q_{p,i}^{n+1}$ are the adsorption/desorption volume, fluid exchange volume, and production/injection volume of node i ; $(m_k)_i^{n+1}$ and $(m_k)_i^n$ is only applicable when $p = g$.

$$F_{p,ij} = \lambda_{p,ij+1/2} T_{ij} (\Phi_{pj} - \Phi_{pi}) \tag{8}$$

$\lambda_{p,ij+1/2}$ is the mobility of the phase p , defined as:

$$\lambda_{p,ij+1/2} = \left(\frac{\rho_p K_{rp}}{\mu_p} \right)_{ij+1/2} \tag{9}$$

where, the subscript $ij + 1/2$ represents the weighted average of the attribute parameters of units i and j .

The connection relationship between two adjacent grids is shown in Fig. 3, which is the conduction coefficient between two adjacent grids. The expression is:

$$T_{ij} = \frac{\alpha_i \alpha_j}{\alpha_i + \alpha_j} \tag{10}$$

$$\alpha_i = A_{i,j} \frac{K_i}{L_i} \mathbf{n}_i \mathbf{f}_i \tag{11}$$

Where, A_{ij} is the interface area of elements i and j , m^2 ; L_i and L_j are the distances from the center point of elements i and j to the interface between elements i and j , m ; $K_{ij+1/2}$ is the absolute permeability of the connection (harmonic average), m^2 .

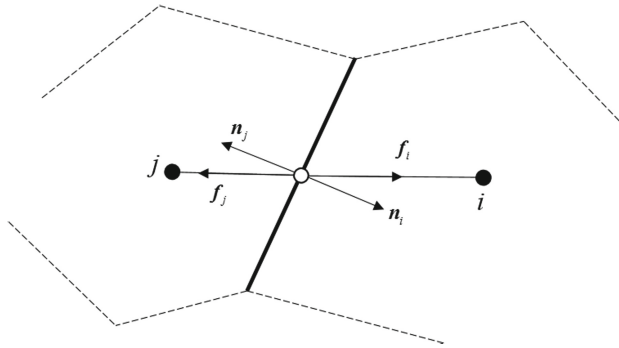


Fig. 3. The relationship between two adjacent grids.

The Peaceman formula [9, 10] is used for the processing of the wellbore item, which is not repeated here.

4 Mathematical Model of Adsorption/Desorption Mechanism

The main difference between shale gas and conventional natural gas reservoirs is that most shale gas is stored in the surface of shale matrix pores in an adsorbed state. Adsorption refers to a very thin molecular layer adhering to the surface of a solid or liquid. The molecular layer is in contact with the surface of a solid or liquid. The surface of the shale reservoir matrix has a strong physical adsorption effect on the gas. During drilling, completion and production, the pore pressure drops, breaking the original adsorption balance, and the gas adsorbed on the matrix surface desorbs. The adsorption of gas on the surface of the shale reservoir matrix particles is mainly affected by temperature, pressure, adsorbate (gas type and property), and adsorbent (reservoir type, specific surface area, solid adsorption capacity).

Brunauer [11] gives five kinds of isothermal adsorption curves. Energy Information Administration report of the US Department of Energy (EIA) [12] gives the adsorption curve of Marcellus shale gas. Comparing the isotherm adsorption curves in the two literatures, it is very similar. This curve is the classic Langmuir isotherm adsorption

curve. The Langmuir isotherm adsorption curve is a curve widely accepted in academy and industry to describe the adsorption characteristics of shale gas [13]. According to the EIA report, when the gas reservoir pressure is below 2,000 psi (13.79 MPa), the desorbed gas is the main component of total natural gas production (50–80%); above 2,000 psi (13.79 MPa), the amount of desorbed gas is also very large, accounting for 30–50% of the total output of natural gas [14]. The curve of the adsorbed gas [12] once again confirmed that the relationship between the gas adsorbed in the shale reservoir and the gas reservoir pressure conforms to Langmuir's law of isotherm adsorption [15].

Langmuir's law of isotherm adsorption can be described according to the following formula [16]:

$$V_E = V_L \frac{P}{P + P_L} \quad (12)$$

Where, V_E is the amount of gas absorbed by the shale per unit mass (t), m^3/t ; V_L is the maximum natural gas adsorption capacity or Langmuir volume, m^3/t ; P_L is the Langmuir pressure, that is the pressure when natural gas adsorption capacity is the 50% of the maximum adsorption capacity, MPa. P is the gas pressure, MPa.

The amount of desorbed gas in the pores of the kerogen matrix in shale reservoirs is controlled by the term m_k in the accumulation term in the main governing Eq. (1). The adsorption volume V_E in Eq. (12) needs to be transformed into the adsorption mass m_k in Eq. (1). The amount of adsorbed gas is determined by the Langmuir isotherm. The adsorbed gas and free gas are in equilibrium. With the production of gas, the pressure in the gas reservoir drops. When the pressure is lower than the equilibrium pressure, the adsorbed gas is desorbed from the surface of the kerogen and becomes free gas. Because the permeability of the matrix is extremely low and the gas velocity inside the kerogen is extremely slow, the speed of desorption is relatively faster. We assume that the adsorption gas and the free gas will reach equilibrium in an instant, that is to say, when the pressure changes, the adsorption or desorption reaction does not have a short delay, and it will be completed in an instant [17].

Therefore, in Eq. (1), the shale matrix model considering the desorption mechanism is:

$$m_k = \rho_R \rho_g V_E \quad (13)$$

Where, m_k is the mass of the adsorbed gas in the reservoir volume V [18], kg; ρ_R is the rock density, kg/m^3 ; ρ_g is the natural gas density in the standard state, kg/m^3 ; V_E is the volume of Langmuir isotherm adsorbed gas, m^3 .

5 Matrix-Fracture-wellbore Mixed Medium Simulation Technology

In the current unconventional shale gas development process, if the conventional development method is adopted, there will be a situation of rapid decline in the initial stage of development, it is difficult to ensure long-term stable production and it is

usually keeping an extremely low recovery rate. With the development of stimulation reservoir volume technology, many large-scale artificial fractures are created, along with the natural fractures in the reservoir, showing a staggered distribution of fractures of different scales and different occurrences. Together with the continuously distributed low-porosity and low-permeability matrix pores in the reservoir, the conditions of the shale gas reservoir are very complicated. Therefore, how to deal with fractures and porous media of different scales with large differences in permeability is a crucial issue in the reservoir simulation of shale gas.

We know that in the process of reservoir numerical simulation, the most important link is the flow process. This flow process includes not only the internal of the reservoir, but also all the flows between the reservoir and the wellbore, as well as inside the wellbore. The flow inside the reservoir involves the flow between the same medium (matrix and matrix, fractures and fractures), as well as the flow between different media (matrix and fractures). Therefore, in view of the above key issues, this paper proposes a method for processing multiple media, that is, mixed media processing technology, which is to discretize all media elements underground, including matrix reservoirs, fractures of various scales, and wellbore to form multiple discrete units. Based on the integral finite difference method, each unit performs fluid exchange with other units in contact with it, and the surrounding units can be of any medium (as shown in Fig. 4). Finally, all fluid exchanges are integrated to find with. In order to be able to accurately determine the relationship between the grids, the connectivity table is used to record the relationship between each unit and other units connected to it. This method is an extension of DFN and treats the wellbore as a medium.

Because it is based on the integral finite difference method, this method does not limit the number of grids around each grid. This technology transforms the focus of the research into a separate relationship between the central grid and each grid. The surrounding grid can be a grid of the same medium, a grid of different media, or a wellbore, so the concept of generalized multiple media is proposed. (See Fig. 4 for the schematic relationship).

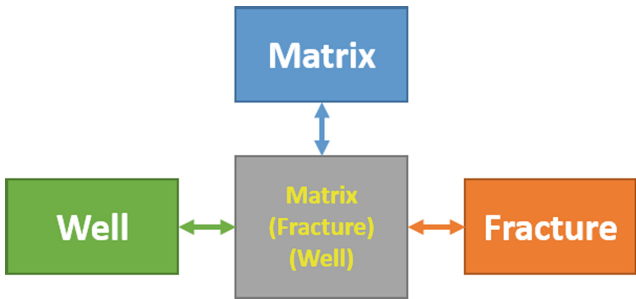
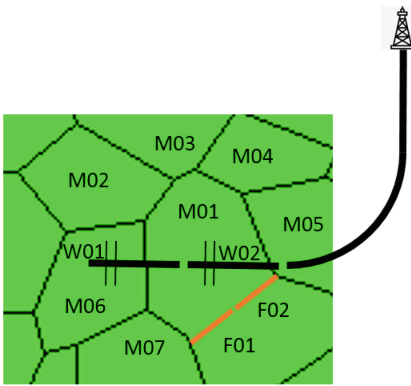


Fig. 4. Conceptual diagram of mixed media.

As shown in the figure above, the gray grid in the center represents the matrix or fracture or wellbore grid. (1) When it is a matrix grid, it can be connected to the same matrix grid (on the right) and can be connected with different fracture grid (lower side), or can be connected to the wellbore grid (left side). (2) When it is a fracture grid, it is similar to the matrix grid, and can be connected to different kinds of matrix grids (right side), can be connected to the fracture grid (lower side) of the same medium, and can also be connected to the wellbore network grid (left). (3) When it is a wellbore grid, for the wellbore processed by the Peaceman analysis method, it can be connected to the matrix grid (right side), and can be connected to the fracture grid (lower side), and can be connected to the wellbore grid (left). (See Fig. 5 for the schematic relationship).



(a) Diagram of relationship between different media

Node <i>i</i>	Node <i>j</i>
M01	M02
M01	M03
M01	M04
M01	M05
M01	M06
M01	M07
M01	F01
M01	F02
M01	W02

(b) Connectivity table

Fig. 5. Schematic diagram of grid connection.

6 Numerical Solution

A fully implicit method combined with Newton-Raphson iteratively solves the system of nonlinear algebraic Eqs. (7). We write the non-linear discrete Eq. (7) in the form of residuals (taking the gas phase as an example, and $(m_k)^{n+1}$, $(m_k)^n$ only applies to the case where $p = g$):

$$R_{p,i}^{n+1} = \left\{ (\phi S_p \rho_p)_i^{n+1} + (m_k)_i^{n+1} - (\phi S_p \rho_p)_i^n - (m_k)_i^n \right\} \frac{V_i}{\Delta t} - \sum_{j \in \eta_i} F_{p,ij}^{n+1} - Q_{p,i}^{n+1} \quad (14)$$

Equation (14) defines a set of $2 \times N$ coupled nonlinear equations. The continuity equations for the two components of gas and water need to be solved separately for each node. In general, the two primary variables of each node need to solve the two related equations by Newton iteration method. The primary variables selected are gas pressure and gas saturation, and other variables such as relative permeability, capillary force, viscosity and density, adsorption term, and the pressure and saturation of non-primary variables are used as secondary variables, and calculated using the formula or relationship table about the change of the primary variable.

As far as the primary variable is concerned, the primary variable residual Eq. (14) of node i is not only a functional relationship of the primary variable of node i , but also a function of the primary variables of all its neighboring nodes j . The Newton iteration method is as follows:

$$\sum_m \frac{\partial R_i^{n+1}(x_{m,l})}{\partial x_m} (\delta x_{m,l+1}) = -R_i^{n+1}(x_{m,l}) \quad (15)$$

Where, x_m is the primary variable of node i and all its neighbors j , $i = 1, 2, 3, \dots, N$, $m = 1$ and 2 ; l is the number of iterations.

The primary variable of Eq. (15) needs to be updated after each Newton iteration,

$$x_{m,l+1} = x_{m,l} + \delta x_{m,l+1} \quad (16)$$

The Newton iteration process continues until the residual $R_{p,i}^{n+1}$ or the amount of change in the primary variable $\delta x_{m,l+1}$ is less than the given error condition.

As described by Y. S. Wu, P. A. Forsyth et al. [19], the numerical method generally forms the Jacobi matrix of Eq. (15). In each Newton iteration loop, Eq. (15) represents a set of $(2 \times N)$ linear coefficient matrix of algebraic equations, iteratively solve linear equations. With the rapid development of computer technology and the gradual refinement of reservoir description, the coefficient matrix of linear algebraic equations has gradually increased in size. Traditional iterative solving techniques have been difficult to ensure the smooth calculation, so this article uses preprocessing solving techniques. That is, the Constrained Pressure Residual solution technology (referred to as CPR solution technology). Based on the decoupling of the Jacobin matrix, for the characteristics of the elliptic equation of the pressure equation and the characteristics of the hyperbolic equation of the saturation equation, the SAMG and BILU methods are used for preprocessing calculations, and then the GMRES method is used for unified solution, which not only guarantees The stability of the calculation also improves the calculation speed, and the details will not be repeated here.

7 Case Study

7.1 Verifying Simulator

Before applying the case, we first need to verify the reliability of this simulator. The verification method used in this article is compared with CMG commercial numerical simulation software. The specific reservoir and fluid static parameters are shown in Table 1.

Table 1. Static parameters of reservoir and fluid.

Physical parameters	Value	Unit
Length of gas reservoir	1000	m
Width of gas reservoir	50	m
Thickness of gas reservoir	90	m
Depth of gas reservoir	2340	m
Permeability of hydraulic fractures	400	mD
Permeability of natural fractures	2.6×10^{-3}	mD
Average permeability of matrix	3.0×10^{-5}	mD
Porosity of hydraulic fractures	0.48%	/
Porosity of natural fractures	0.48%	/
Average porosity of matrix	4.34%	/
Compression coefficient of matrix	1.82×10^{-4}	MPa ⁻¹
Compression coefficient of natural fractures	1.82×10^{-4}	MPa ⁻¹
Initial pressure	38.2	MPa
Initial temperature	323	K
Average initial S_w	42.7%	/
Viscosity of gas	1.84×10^{-5}	cP
Average spacing of hydraulic fractures	26	m
Length of horizontal well	900	m
Number of hydraulic fractures	33	/
Half-length of hydraulic fractures	25	m

For the gas-water two-phase fluid, the production mode adopts a daily gas production of $3 \times 10^4 \text{m}^3/\text{day}$. After 730 days of production, it is then converted to a BHP of 7 MPa for a total of 11322 days. Comparing the values of daily gas production and bottom BHP, the comparison results are shown in Fig. 6

It can be seen from the above figure that the calculation results of the simulator in this paper are consistent with the calculation results of the CMG software, indicating that the simulation results of this simulator are correct and credible.

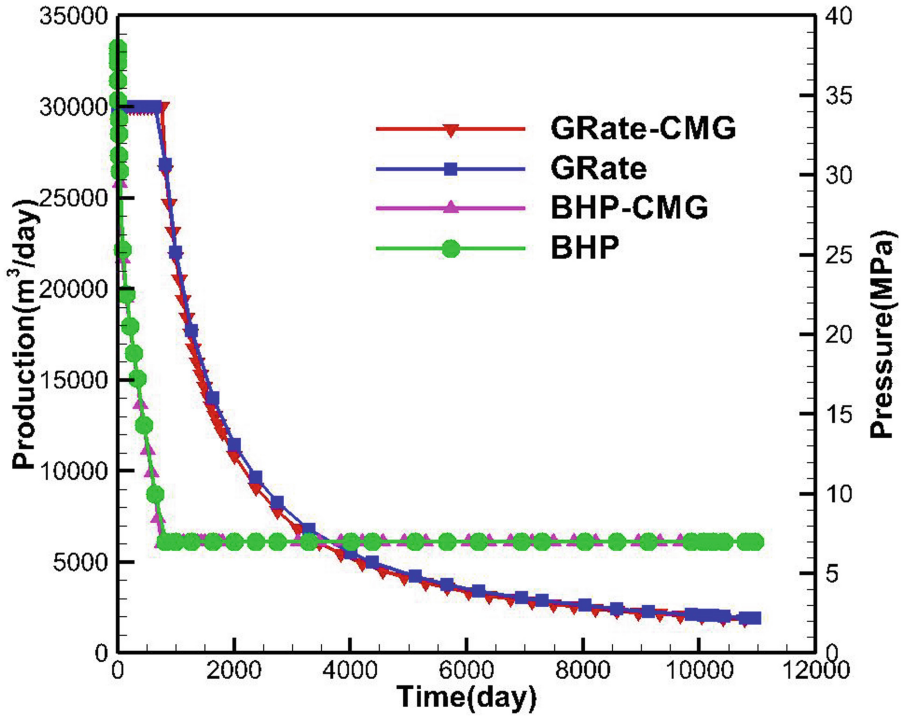
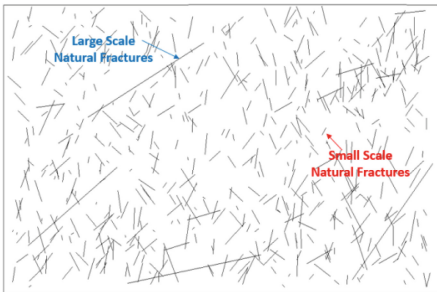


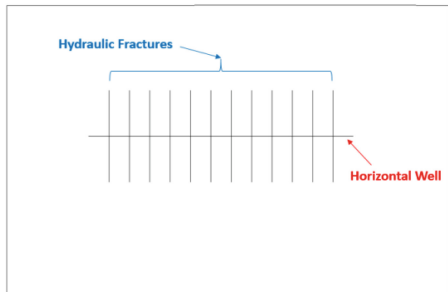
Fig. 6. Comparison with commercial numerical simulation software CMG.

8 Case Study

In view of the complex shale reservoirs with different scale fractures shown in Fig. 7 (a), a horizontal well and 12 sections of hydraulic fracturing fractures were developed and produced in this paper to form the well location and artificial fracture distribution map shown in Fig. 7(b).



(a) Shale reservoirs with complex fractures of different scales



(b) Single horizontal well and artificial hydraulic fracturing fractures

Fig. 7. Shale reservoirs with complex fractures of different scales and the horizontal well and artificial hydraulic fracturing fractures.

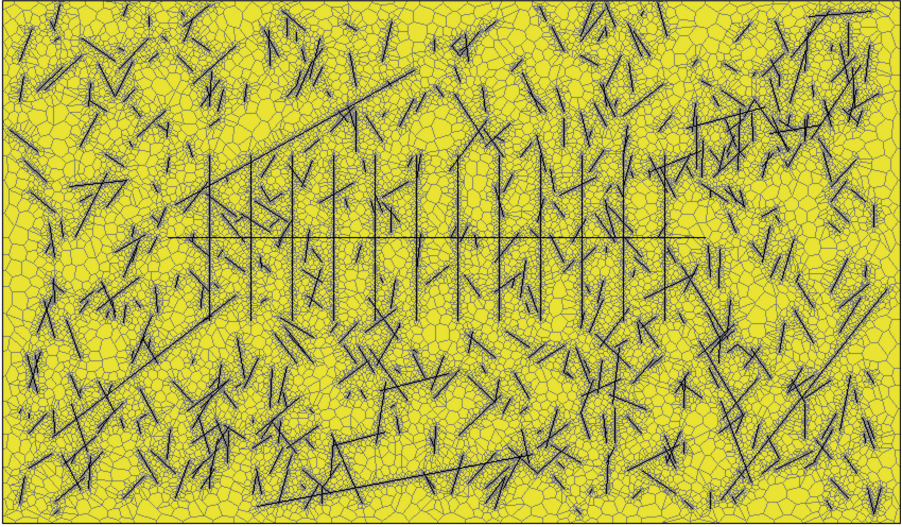


Fig. 8. Sectional view of polygonal unstructured grid.

A polygonal unstructured grid is used to divide the fractures and matrix in the computing domain at different scales. The total number of grids is about 150,000. The specific grid division is shown in Fig. 8. The equilibrium method is used for initialization of all reservoir. The static parameters of the reservoir and fluid are shown in Table 2.

Table 2. Static parameters of reservoir and fluid.

Physical parameters	Value	Unit
Length of gas reservoir	2170	m
Width of gas reservoir	1261	m
Thickness of gas reservoir	20	m
Depth of gas reservoir	3005	m
Permeability of hydraulic fractures	100	mD
Permeability of large scale natural fractures	10	mD
Permeability of small scale natural fractures	1	mD
Average permeability of matrix	1.0×10^{-2}	mD
Porosity of hydraulic fractures	0.5%	/
Porosity of large scale natural fractures	0.5%	/
Porosity of small scale natural fractures	0.5%	/
Average porosity of matrix	10%	/

(continued)

Table 2. (continued)

Physical parameters	Value	Unit
Compression coefficient of natural fractures	1.82×10^{-4}	MPa^{-1}
Compression coefficient of matrix	1.82×10^{-4}	MPa^{-1}
Initial pressure	45	MPa
Initial temperature	323	K
Average initial S_w	16%	/
Viscosity of gas	1.84×10^{-5}	cP
Number of hydraulic fractures	12	/
Half-length of hydraulic fractures	200	m
Average spacing of hydraulic fractures	100	m
Length of horizontal well	1300	m
Langmuir pressure	15.76	MPa
Langmuir volume	6.2×10^{-3}	m^3/kg

For shale gas reservoirs, gas-water two-phase simulation is adopted, the production mode is fixed BHP production, the BHP is 5 MPa, and the total production is 5970 days. The gas-water two-phase infiltration curve used in this paper is shown in Fig. 9.

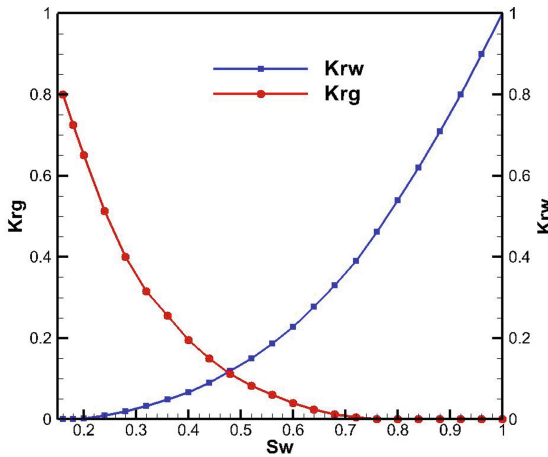


Fig. 9. Gas-water two-phase relative permeability curve.

Figure 10 shows the distribution of reservoir pressure at 30 days, 120 days, 300 days, 900 days, 1440 days, 2610 days, 3600 days and 5970 days. It can be seen from the figure that in the early stage of production, shale gas near artificial hydraulic fractures is first used passively. As production progresses, due to the higher permeability of natural fractures of different scales, the shale gas near the fractures was gradually developed. Due to the extremely low permeability of the shale reservoir matrix, at 5970 days of production, there are still unused areas in areas far from the artificial hydraulic fractures.

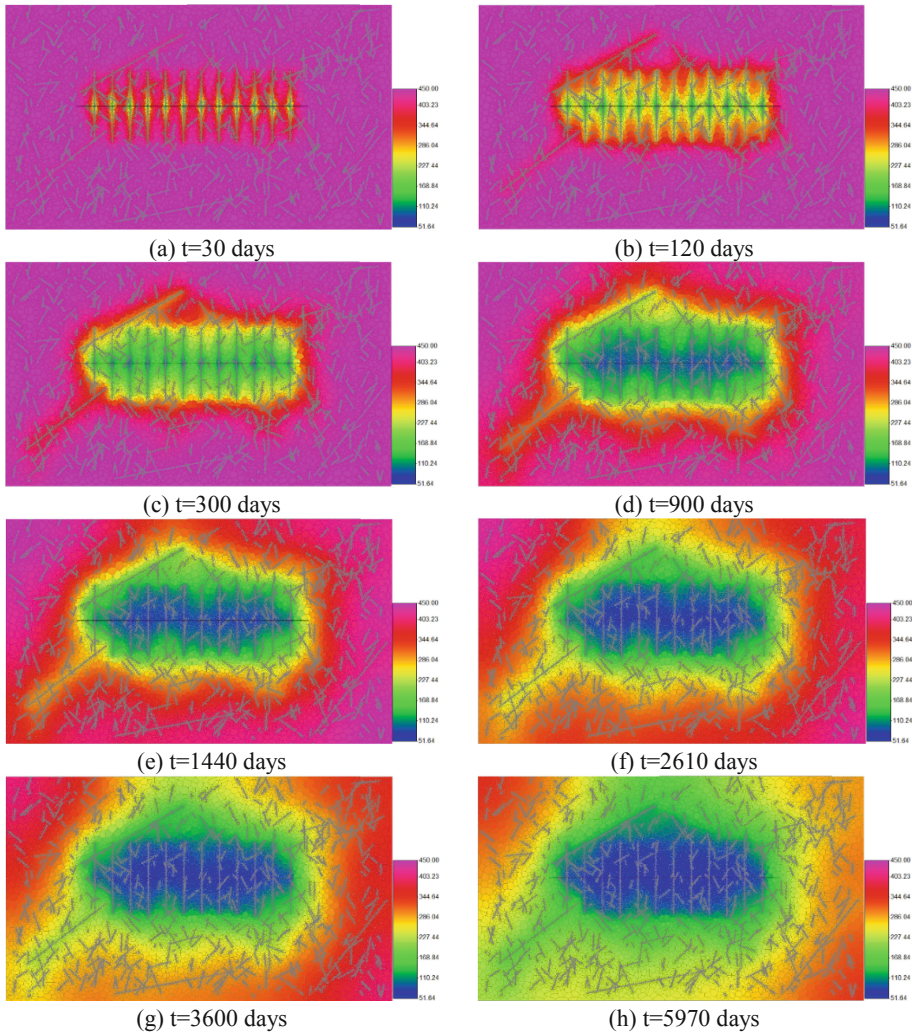


Fig. 10. Pressure distribution of gas reservoir at different times.

Figure 11 shows the cumulative gas production and BHP over time. It can be seen from the figure that due to the high initial reservoir pressure, after 5970 days of production, the pressure gradually decreased from 45MPa to about 20MPa, but the set bottom hole flow pressure of 5MPa has not yet been reached, so the constant BHP production can be maintained. Cumulative gas production has maintained steady growth under conditions of constant pressure production.

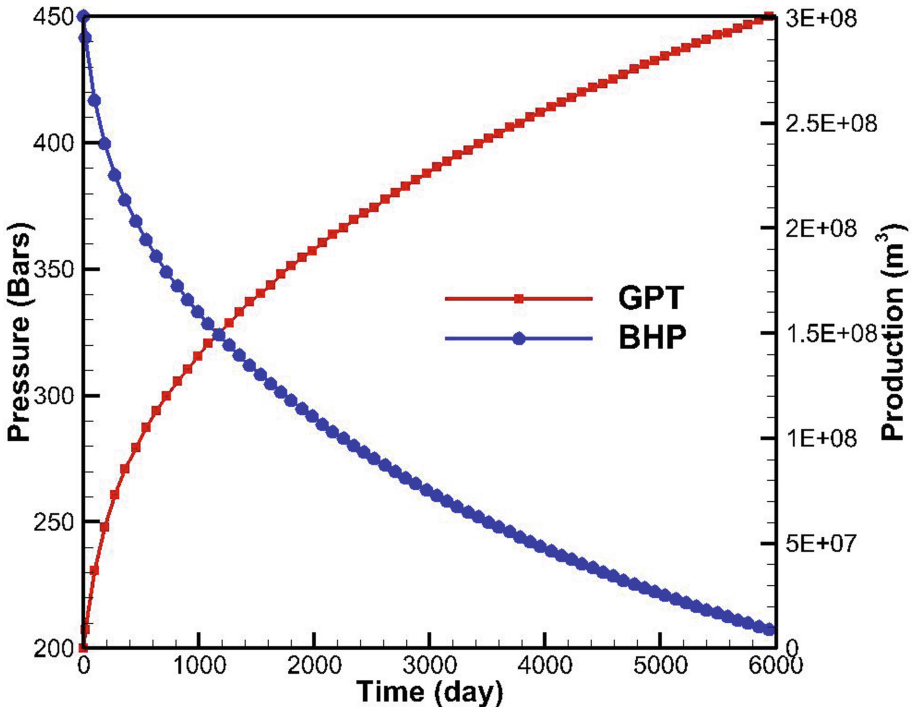


Fig. 11. Cumulative gas production and BHP as a function of time.

9 Conclusions

In order to solve the problems of tight pores, extremely low permeability, complicated gas occurrence state and migration mechanism of shale gas reservoirs, this paper systematically analyzes and summarizes the mechanism and law of adsorption/desorption with shale gas, and establishes a mechanism to consider adsorption/desorption mechanism. Mathematical model of nonlinear migration of shale gas reservoirs, a matrix-fracture-wellbore mixed medium simulation technology was constructed, a shale gas numerical simulator was developed and verified by comparison with commercial software calculation results. The model, method and simulator are correct and credible. Finally, the numerical simulation calculation of shale gas migration considering the adsorption mechanism is carried out. From the numerical simulation results, it can be seen that the mixed medium simulation technology can effectively simulate the complex flow of shale gas. This technology is suitable for direct numerical simulation calculation of shale gas development, and provides powerful numerical simulation techniques for gas field development workers.

Acknowledgments. The project is supported by the Research on integrated mathematical model of fracture network and software module development RIPED Project (Number YGJ2019-07-04).

References

1. MIT (Massachusetts Institute of Technology), The Future of Natural Gas – An Interdisciplinary MIT Study, (Updated from 2010 version) (2011)
2. Yuewei, F.: Research on american shale gas development strategy-american shale gas dream (Chinese). *Int. Pet. Econ.* **1**, 92–100 (2012)
3. Chengzao, J., Min, Z., Yongfeng, Z.: China's unconventional oil and gas resources and prospects for exploration and development (Chinese). *Pet. Explor. Dev.* **2**, 129–136 (2012)
4. EIA (U.S. Energy Information Administration), Annual Energy Outlook 2020: Early Release Reference Case, AEO2020 Early Release Rollout Presentation, Washington, DC (2020)
5. Chang, L.: The enlightenment of American “shale gas revolution” to China (Chinese). *Pet. Knowl.* **6**, 60 (2012)
6. Hai, S., Jun, Y., Zhixue, S., et al.: Progress and prospect of shale gas numerical simulation technology (Chinese). *Oil and Gas Geol. Recovery Effi.* **19**(1), 46–49 (2012)
7. Zhang Yuandi, Y., Gaoming, S.G., et al.: Investigation on numerical simulation technology of shale gas reservoirs abroad (Chinese). *Oil Gas Field Dev. Exploit.* **10**(3), 40–43 (2012)
8. Narasimhan, T.N.: An integrated finite difference method for analyzing fluid flow in porous media. *Water Resour. Res.* **12**(1), 57–64 (1976)
9. Peaceman, D.W.: Interpretation of well-block pressures in numerical reservoir simulation with nonsquare grid blocks and anisotropic permeability. In: paper SPE-10528 presented at Sixth SPE Symposium on Reservoir Simulation, Soc. of Pet. Eng., New Orleans, La., (1982)
10. Peaceman, D.W.: Representation of a horizontal well in numerical reservoir simulation. In: paper SPE-21217 presented at 11th SPE Symposium on Reservoir Simulation, Soc. of Pet. Eng., Anaheim, Calif. (1991)
11. Stephen Brunauer, P.H., Emmett, E.T.: Adsorption of gases in multimolecular layers. *J. Am. Chem. Soc.* **60**(2), 309–319 (1938). <https://doi.org/10.1021/ja01269a023>
12. EIA (U.S. Energy Information Administration), World Shale Gas Resources: An Initial Assessment of 14 Regions Outside the United States (2011)
13. Silin, D., Kneafsey, T.: Gas shale: from nanometer-scale observations to well modeling. In: CSUG/SPE 149489, presented at the Canadian Unconventional Resources Conference, Calgary, Alberta, Canada (2011)
14. Mengal, S.A., Wattenbarger, R.A.: Accounting for adsorbed gas in shale gas reservoirs. *SPE* 141085 (2011)
15. Liping, Z., Renfang, P.: The main elements of shale gas accumulation and gas storage transformation (Chinese). *China Pet. Explor.* **3**, 20–23 (2009)
16. Langmuir, I.: The constitution and fundamental properties of solids and liquids. *J. Am. Chem. Soc.* **38**(11), 2221–2295 (1916)
17. Moridis, G.J., Blasingame, T.A., Freeman, C.M.: Analysis of mechanisms of flow in fractured tight-gas and shale-gas reservoirs. In: SPE 139250, presented at the SPE Latin American & Caribbean Petroleum Engineering Conference held in Lima, Peru (2010)
18. Leahy-Dios, A., Das, M., Agarwal, A., Kaminsky, R.D.: Modeling of transport phenomena and multicomponent sorption for shale gas and coalbed methane in an unstructured grid simulator. In: SPE 147352, presented at the SPE Annual Technical Conference, Denver, Colorado (2011)
19. Wu, Y.S., Forsyth, P.A., Jiang, H.: A consistent approach for applying numerical boundary conditions for multiphase subsurface flow. *J. Contam. Hydrol.* **23**, 157–184 (1996)